



EFFECT OF CELL GEOMETRY ON THE DENDRITIC ELECTRODEPOSITS OF COPPER

Talal Ahmed S.K.¹, Dr.Shaikh Gazala Farheen², A.R.khan³ and Gulam Rabbani⁴

¹Research student Maulana Azad College Aurangabad Maharashtra India.

²Lecturer, Deogiri College, Aurangabad, Maharashtra, India.

³HOD, PG Department of Computer Science, Maulana Azad College, Aurangabad, Maharashtra India.

⁴Director, Dr.Rafiq Zakaria Centre for Higher learning and advanced Research, Aurangabad, Maharashtra India.

ABSTRACT

Electrodeposition is studied using three different cell geometries i.e. circular, square and triangular cell geometry. The electrodeposition of metal ions in an electrolytic cell is governed by Diffusion (DLA) like processes and therefore the effect of applied electric field and the distribution of electric field ultimately governs the shape of electrodeposit under a given set of working conditions determined by the properties of electrolyte and the working temperature. We present the findings related to the deposition of dendritic patterns from copper sulphate solution under different geometries.

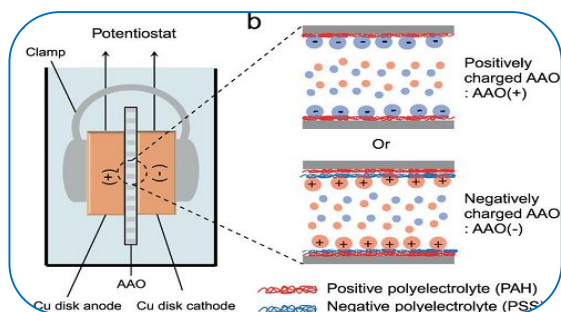
KEYWORDS: Electro-deposition, copper- sulphate , fractal, fractal dimension, Diffusion Limited Aggregation, Box counting

1. INTRODUCTION:

The Electrodeposition from electrolyte solutions is governed by DLA like conditions at room temperature^{1, 2, 3} where two driving forces are simultaneously acting on the ions in the electrolyte. When a solute like copper sulphate CuSO_4 is dissolved in water it decomposes into constituent ions^{4, 5}



When the electrolyte is subjected to an electric field of strength E , the ions experience a force in the direction of electric field whose strength is qE where q is the charge on the ion. Under the conditions when the size of the electrodeposit becomes comparable with the electrode spacing, the strength of electric field keeps changing from time to time as the growth proceeds, also depending on the shape of the electrodes there are regions of different electric field. The electrostatic force resulting from the electric field acting on



the ionic charges makes the charges move towards the respective electrodes i.e. the positive charges tend to move towards the cathode and the negative charges move towards the anode. In a circular cell geometry, there is a circular anode at the centre of which a point cathode is situated and the space between the cathode and anode is filled with the electrolyte solution. The ions, Cu^{++} and SO_4^{-} experience a force towards cathode and anode respectively and thus metallic copper deposits at the cathode and SO_4 ions are liberated at the anode and

if the anode is made of copper this results in formation of CuSO_4 again which is responsible for keeping the concentration unchanged.

EXPERIMENTAL SECTION

At room temperature there is a constant random motion associated with the particles of the electrolyte including the two ions. This zigzag random motion also known as Brownian motion is super imposed on the drifting of ions under the influence of electric field and therefore such an Electrodeposition which is limited by diffusion of the ions because of Brownian motion is known as Diffusion Limited Aggregation (DLA) and exhibits fractal character^{6,7,8,9}. In the circular cell geometry, at the commencement of the Electrodeposition there is a strong electric field at the central cathode and thus there is strong growth all around the point cathode giving it appearance of a small lump. As the growth proceeds the point that are already grown tend to be nearer to the outer anode and stand higher probability of sticking a metal ion as compared to the nearby regions. This suggested the study of electrodeposits in different cell geometry, therefore we studied Electrodeposition in three different cell geometries i.e. circular, square and triangular^{10,11}.

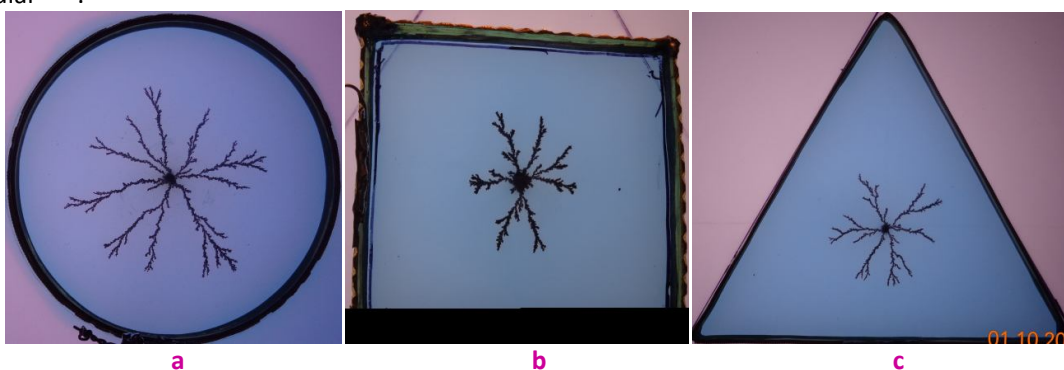


Fig. 1 Electrodeposition cells with circular, square and triangular geometry.

Three different Electrodeposition cells were constructed using copper strips as outer anode formed into a shape of circle, square and triangle respectively and were mounted on a sheet of acrylic. At the centre of the outer copper anode a small hole (0.8 mm diameter) was drilled in the acrylic sheet to accommodate a pin acting like a point cathode. The cell operating voltage was kept constant at 9 V DC regulated and the electrolyte used was 1 Molar CuSO_4 solution as the electrodeposits under these operating conditions were reproducible in morphology. The three fully developed electrodeposits are shown in Fig. 1, the electrodeposits if allowed to grow further, approaching the anode the electric field conditions become too much different resulting in excess of branching. For the characterization of the shape of electrodeposits the images shown in Fig. were converted to two color bitmaps as shown in Fig. 2.

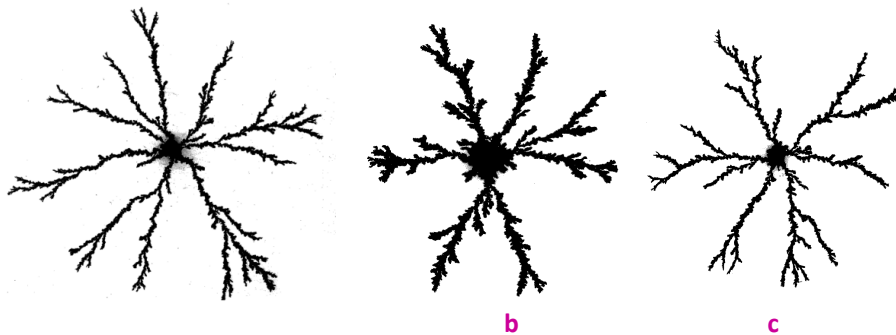


Fig. 2 Two color bitmap images obtained from images of Fig. 1 corresponding to circular, square and triangular cell geometry.

The two color bitmap images of Fig. 2 were analysed for fractal dimension using box counting technique implemented using a computer program to count the total number of boxes (N) required to completely cover the image using square boxes of different sizes (r).

Circular cell geometry:

A typical electrodeposit obtained from 1 M copper sulphate solution in a circular Electrodeposition cell operating at 9 V is shown in Fig. 1 (a) and its two color bitmap is shown in Fig. 2 (a). The results of box counting applied to the image of Fig. 2 (a) is shown in Table – 1.

The data from Table – 1 is used to plot a graph of $\log(N)$ versus $\log(r)$ as shown in Fig. 3 using $\log(r)$ on the axis of x and $\log(N)$ on the y-axis. The points plotted in the form of small circles represent the actual data taken from Table – 1. It is seen that all the points lie well along a straight line indicating that the power law holds good and self-similarity is present confirming that the pattern analysed is a fractal. The data points are fitted to a straight line using the method of least squares and the best fitting straight line is also shown joining these points and the equation of the best fitting straight line is also given in the inset. The slope of the straight line is used for the estimation of Fractal Dimension as $D = -\text{Slope}$.

Table – 1: Results of box counting applied to image of Fig. 2 (a).

R	N	$\log(r)$	$\log(N)$	r	N	$\log(r)$	$\log(N)$
1	69239	0	4.8404	34	253	1.5315	2.4031
2	20399	0.301	4.3096	39	213	1.5911	2.3284
3	10307	0.4771	4.0131	44	183	1.6435	2.2625
4	6505	0.6021	3.8132	50	155	1.699	2.1903
5	4464	0.699	3.6497	57	124	1.7559	2.0934
6	3342	0.7782	3.5240	64	113	1.8062	2.0531
7	2626	0.8451	3.4193	72	96	1.8573	1.9823
8	2174	0.9031	3.3373	81	77	1.9085	1.8865
9	1784	0.9542	3.2514	91	66	1.959	1.8195

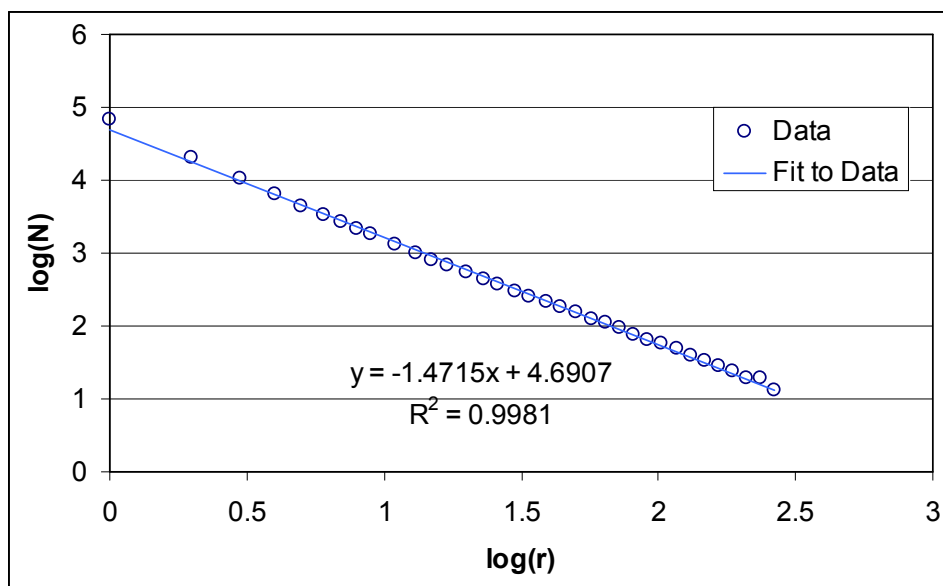


Fig. 3 $\log(N)$ versus $\log(r)$ plot of data from Table – 1 corresponding to Fig. 1 (a) and 2(a) showing fractal dimension of 1.4715.

It is seen from Fig. 1 that the geometry being symmetric in circular cell more or less all the branches tend to originate from the central cathode in outward direction with formation of secondary branches. In circular cell geometry, the region between two neighboring branches shows the least growth as there is very little chance for the wandering ions to enter this region before sticking to the nearby branches, such a effect is called as masking effect.

SQUARE CELL GEOMETRY:

In square cell geometry, the conditions in the cell are not symmetric as are in the circular cell. The electric field not uniform or symmetric as the corners of the outer anode are at a higher distance from the central cathode as compared to the other portions of the anode. The four boundaries that are nearer the central cathode as compared to the corners tend to affect more and the branch formation is favored in these directions. Fig. 1 (b) shows that the branches proceed in towards the straight boundaries and two prominent branches are seen in the direction of each side of the square.

Table – 2: Results of box counting applied to image of Fig. 2 (b).

R	N	log(r)	log(N)	r	N	log(r)	log(N)
1	148992	0	5.1732	39	241	1.5911	2.382
2	41491	0.301	4.618	44	211	1.6435	2.3243
3	19401	0.4771	4.2878	50	169	1.6990	2.2279
4	1149	0.6021	4.0588	57	138	1.7559	2.1399
5	7610	0.6990	3.8814	64	117	1.8062	2.0682
6	5465	0.7782	3.7376	72	99	1.8573	1.9956
7	4189	0.8451	3.6221	81	87	1.9085	1.9395
8	3327	0.9031	3.5221	91	69	1.9590	1.8388
9	2699	0.9542	3.4312	103	58	2.0128	1.7634
11	1901	1.0414	3.279	116	51	2.0645	1.7076
13	1424	1.1139	3.1535	131	42	2.1173	1.6232
15	1132	1.1761	3.0538	147	35	2.1673	1.5441
17	931	1.2304	2.9689	165	30	2.2175	1.4771
20	709	1.3010	2.8506	186	27	2.2695	1.4314
23	552	1.3617	2.7419	209	22	2.3201	1.3424
26	460	1.4150	2.6628	235	15	2.3711	1.1761

For one side, the two branches started initially, however due to masking effect one of the two branches (the upper one) got retarded and thus the growth of that branch is stopped and remained dwarf. The two color bitmap of image from Fig. 1(b) is shown in Fig. 2 (b) and the results of box counting implemented to this image are given in Table – 2. Using the log(N) and log(r) data from this table a graph is plotted using log(r) on the x-axis and log(N) on the axis of y as shown in Fig. 4.

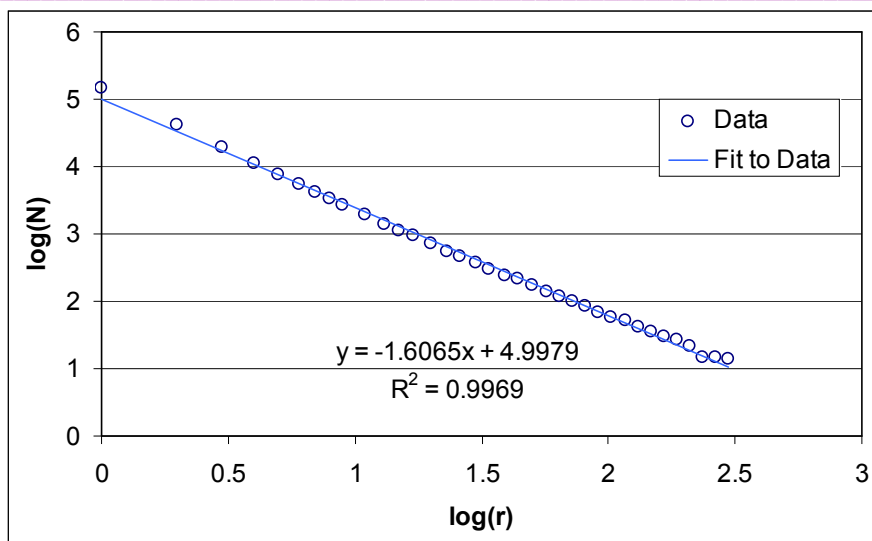


Fig. 4 $\log(N)$ versus $\log(r)$ plot of data from Table – 2 corresponding to Fig. 1 (b) and 2 (b) for square cell showing fractal dimension of 1.6065.

In Fig. 4 the points plotted represent actual data from Table – 2 and the straight line joining these points is the best fitting straight line to this data whose equation is shown in the inset of the plot. The fractal dimension obtained from the slope of the straight line is 1.6065 indicating slightly higher degree of complexity with the shape of the electrodeposit as compared to that in circular cell geometry.

Triangular cell geometry:

The case of triangular cell geometry is slightly different from the square cell geometry, again here there is a tendency of the branches to grow towards the straight edges of the outer anode. For all the three sides of the triangle, two branches are growing in the direction of each of the side with a tendency to avoid growth towards corners of the triangular anode. Again here the effect of masking is clearly visible as growing branches continue to grow and no appreciable electrodeposit is seen in the region between the two branches. These electrodeposits are also representatives of true DLA like growth with that there is more likelihood of development of the branches towards the sides of the triangle. The electrodeposit obtained using triangular cell geometry with 1 Molar copper sulphate as an electrolyte and a cell operating voltage of 9 V DC regulated is shown in Fig. 1 (c) whose two color bitmap equivalent is shown in Fig. 2 (c).

For the purpose of fractal analysis the two color bitmap of Fig. 2 (c) obtained from Fig. 1(c) is subjected to box counting using computer program that counts the total number of boxes (N) required to completely cover the image using square boxes of different sizes (r). The results of box counting implemented to the image shown in Fig. 2 are presented in Table – 3.

Table – 3: Results of box counting applied to image of Fig. 2 (c).

R	N	$\log(r)$	$\log(N)$	r	N	$\log(r)$	$\log(N)$
1	74535	0	4.8724	39	192	1.5911	2.2833
2	21919	0.301	4.3408	44	162	1.6435	2.2095
3	10650	0.4771	4.0273	50	141	1.699	2.1492
4	6493	0.6021	3.8124	57	118	1.7559	2.0719
5	4444	0.699	3.6478	64	100	1.8062	2

6	3269	0.7782	3.5144	72	90	1.8573	1.9542
7	2533	0.8451	3.4036	81	72	1.9085	1.8573
8	2068	0.9031	3.3156	91	60	1.959	1.7782
9	1701	0.9542	3.2307	103	54	2.0128	1.7324
11	1254	1.0414	3.0983	116	47	2.0645	1.6721
13	963	1.1139	2.9836	131	39	2.1173	1.5911
15	776	1.1761	2.8899	147	35	2.1673	1.5441
17	638	1.2304	2.8048	165	27	2.2175	1.4314
20	499	1.301	2.6981	186	23	2.2695	1.3617
23	402	1.3617	2.6042	209	20	2.3201	1.301
26	338	1.415	2.5289	235	18	2.3711	1.2553
30	282	1.4771	2.4502	264	14	2.4216	1.1461
34	237	1.5315	2.3747	297	13	2.4728	1.1139

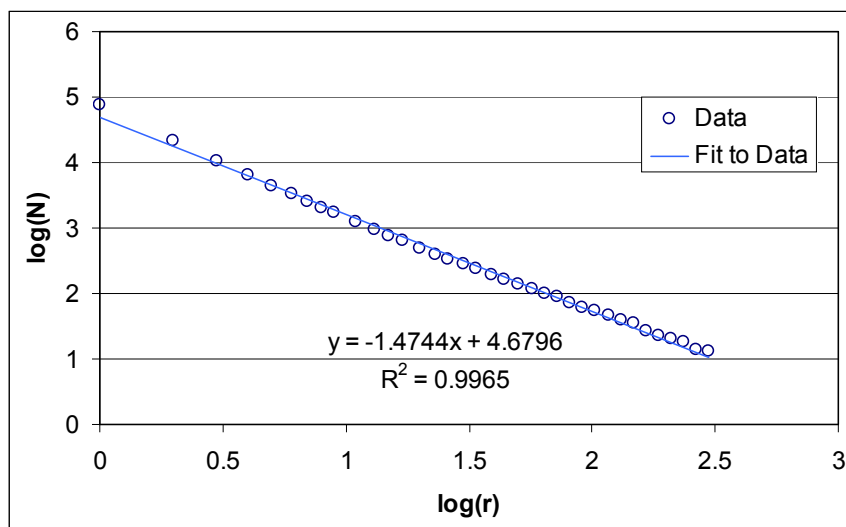


Fig. 5 $\log(N)$ versus $\log(r)$ plot of data from Table – 3 corresponding to Fig. 1 (c) and 2 (c) for Triangular cell shows in fractal dimension of 1.4744.

A graph is plotted using the values of $\log(N)$ and $\log(r)$ from Table – 3 as shown in Fig. 5. The points plotted represent the actual data from Table – 3 and the straight line joining these points is the best fitting straight line to the data obtained using the method of least squares whose equation is also shown in the inset. The fractal dimension of the shape of the electrodeposit obtained using circular cell geometry is 1.4744.

RESULTS AND DISCUSSIONS / CONCLUSION

A comparison of the fractal dimension of the electrodeposits obtained from 1 M copper sulphate solution as an electrolyte is given in Table – 4.

Table – 4 : Comparison of Fractal Dimensions of the image shown in Fig. 1

S. No.	Cell Geometry	Slope	Fractal Dimension	R ²
1	Circular	-1.4715	1.4715	0.9981
2	Square	-1.6065	1.6065	0.9969
3	Triangle	-1.4744	1.4744	0.9965

Table – 4 shows that the fractal dimensions of all the three patterns obtained from three different cell geometries under similar operating condition are close to the DLA value which is 1.6. The value of fractal dimensions for circular and triangular cell geometries are close to each other around 1.47 where as that for the square cell geometry it is about 1.6. The reason is that the interior region in the triangular cell geometry resembles conditions in the circular cell except for the edges and thus the electrodeposit of square cell geometry exhibits a higher fractal dimension of 1.6065 which is close to the DLA fractal dimension.

REFERENCES

1. I. Mogi, M.Kamiko and S.Okubo, 'Magnetic field effects on fractal morphology in electrochemical deposition', *Physica B: Condensed Matter*, Issues 1–4, 1 May 1995, Volume 211, Pages 319-322.
2. Vincent Fleury, 'Branched fractal patterns in non-equilibrium electrochemical deposition from oscillatory nucleation and growth', *Nature*, 13 November 1997 volume 390, pages 145–148.
3. Sander Leonard M., 'Fractal Growth,' *Scientific American*, 94 (1987).
4. Sander L. M., 'Diffusion Limited Aggregation,' *Contemporary Physics*, 2000, vol 41, pages 203.
5. Witten T. & Sander L. M., *Phys Rev Lett*, 1981, vol 47, pages 1400.
6. Meron EHUD, *Phys Rep*, vol 1, pages 218 .
7. Cross M C & Hohenberg P C, *Rev Mod Phys*, 1993, vol 65, pages 851.
8. Family F. & Landau D. P. edited '*kinetics of aggregation and gelation*' (Noth-Holland, Amsterdam) 1984.
9. Starzyk C F, *Polimery*, 37, 298 (1992).
10. Heinz O.P, Hartmut J. and Diemar S., 'Chaos and Fractals' *New Frontiers of Science*, 697(New York: Springer-Verlag)(1992).
11. Pablo F.J. Deleon, Ezequiel v. Albano, and Salvarezza R.C., ' Interface dynamics of copper electrodeposition *Phys Rev E* 66, 042601(2002).